Int. J. Morphol.,
39(5):1487-1492, 2021.

Estimating Glenoid Fossa width for Instability-related Bone loss with CT Scan in a Chilean Sample

Estimación del Ancho de la Fosa Glenoidea para la Pérdida Ósea Relacionada con Inestabilidad con Tomografía Computarizada en una Muestra Chilena

Julio Contreras[1,2,3,4]; Claus Ogrodnik[2] & Pablo Khek[2]

CONTRERAS, J.; OGRODNIK, C. & KHEK, P. Estimating glenoid fossa width for instability-related bone loss with CT scan in a Chilean sample. *Int. J. Morphol., 39(5)*:1487-1492, 2021.

SUMMARY: Glenoid fossa bone loss has been associated with recurrence and failure after glenoid labrum repair for shoulder instability. Quantification of glenoid fossa bone loss is critical for the successful treatment of glenohumeral instability. The aim of this paper was to estimate a linear regression model based on glenoid height in CT scan adjusted for age and sex to calculate glenoid fossa width in a healthy Chilean sample. CT scans of 101 shoulders were reviewed. The mean age was 51.96 years (SD 19.16; range, 15–88 years) with 53 females and 48 male patients. Studies with signs of bone loss, instability, fracture, or arthritis were excluded. After 3D-CT reconstruction, the height and width of each glenoid fossa was measured using the Owens methodology. All landmarks for the 2 measurements were placed on the most lateral surface of the glenoid fossa margin. Measurements for all shoulders were recorded by 3 observers and repeated on a subset (n = 20) of shoulders, under blinded conditions, by the same observer, at least 2 weeks after the initial measurements. Descriptive statistics, intraclass correlation and regression coefficients were calculated with Stata BE 17® software. A p-value of 0.05 was considered significant. A linear regression model was estimated resulting in the formula "Width = 10.97 + 0.02 * Age + 0.41 * Height - 1.95 * Sex (1=Female, 0=Male)". This model presented all coefficients with $p < 0.05$ and an adjusted R2 of 0.73. Furthermore, it fulfilled the assumption of linearity, normal distribution of errors, independence of errors, and homoscedasticity. Regarding the intraobserver correlation, ICC was 0.76 for height and 0.91 for width; the interobserver ICC was 0.93 for height and 0.86 for width. A 3D-CT specific formula was developed to predict glenoid fossa width based on height with sufficient accuracy to be clinically valuable.

KEY WORDS: Shoulder joint; Glenoid fossa; Anatomy; Shoulder dislocation.

INTRODUCTION

Glenoid, humeral, or bipolar bone defects are risk factors for recurrence associated with glenohumeral instability (Park *et al*., 2020; Apostolakos *et al*., 2021). Since 2000, Burkhart & de Beer (2000) have identified "glenoid bone deficit" as independent risk factors for glenoid labrum repair failure describing the "inverted pear-glenoid". However, the diagnosis of bone defects was made intraoperatively, and their condition as a "engaging" lesion was evaluated. In 2002, Burkhart *et al*. (2002) described a method to quantify glenoid bone loss arthroscopically.

Preoperative imaging studies are key for decision-making and planning (De Filippo *et al*., 2020; Stefaniak *et al*., 2020). There are several modalities, but CT scans are the most suitable to evaluate the glenoid bone defect (Zhang *et al*., 2020). However, there are many methods described to estimate the size of the glenoid bone defect (Provencher *et al*., 2010). The most commonly used are the surface area method, the superimposed circle method, the PICO method, and the bare area method (Willemot *et al*., 2018).

Giles *et al*. (2015) described the use of glenoid height to estimate its width and thus evaluate the glenoid bone defect. The bone defect is generally anterior affecting the width of the glenoid but does not affect its height. The height of the glenoid and its relationship with the glenoid fossa width is relatively constant at the population level. However, the effect of age, sex, and specific population characteristics can affect its reproducibility. The purpose of this study was to estimate a linear regression model based on glenoid height

[1] Shoulder and Elbow Unit. Instituto Traumatológico, Santiago, Chile.
[2] Department of Orthopedics and Trauma. Universidad de Chile, Santiago, Chile.
[3] Shoulder and Elbow Unit. Pontificia Universidad Católica de Chile, Santiago, Chile.
[4] Department of Orthopedics and Trauma. Pontificia Universidad Católica de Chile, Santiago, Chile.

in CT scan adjusted for age and sex to calculate glenoid fossa width in a healthy Chilean sample. Thus, we reviewed 101 CT scans from our institutional database to analyze glenoid anatomy.

MATERIAL AND METHOD

Sample. CT scans of 214 shoulders from our institutional database were reviewed to analyze the anatomy of the glenoid excluding studies with incomplete images, poor quality, artifacts, or signs of structural, traumatic, or degenerative changes (bone loss, instability, fracture, arthritis, or any alteration of the glenoid anatomy); 101 CT scans were finally processed. The mean age was 51.96 years (SD 19.16; range, 15–88 years) with 53 females and 48 male patients.

CT data acquisition and processing. Patients were scanned in a Siemens SOMATOM® Volume Zoom (Siemens Medical Solutions USA, Malvern, PA). The patients were placed in a supine anatomic position (Gantry tilt 0°), and images were obtained in 1–mm increments (Slice collimation 4 ¥ 1 mm) along the axial axis of the human body. The images were acquired at 140 kVp and 150 mA with a 250-mm field of view (FOV), 512 matrix resolution, and rotation speed of 0.75 s per revolution. The FOV of each scan included the entire scapula. Images were processed with RadiAnt DICOM Viewer® 2020.1.1.

Morphometric measurements. Two morphometric measurements were obtained for each of the scapulae: height and width. The height and width were measured based on the methodology published by Owens *et al*. (2013); the glenoid height was measured as the maximum length from the upper pole of the glenoid (12 o'clock position) to the lower pole (6 o'clock position), and the glenoid fossa width was measured as the maximum diameter in an orthogonal orientation to the previously measured height (Fig. 1). All landmarks for both measurements were placed on the most lateral surface of the glenoid fossa margin. To perform the measurements, a three-dimensional reconstruction (3D-CT) with RadiAnt DICOM Viewer® 2020.1.1 was performed after subtraction of the humeral head. Reconstruction is positioned obtaining a true "en face" view when the image displays the glenoid articular surface with its largest surface extension in the horizontal and vertical planes (Zhang *et al*.).

Analysis of CT images. All images were measured by a shoulder and elbow surgeon (5 years of practice and 10 years of experience) and two orthopedics residents. Forty CT scans were re-evaluated in a blinded mode with at least two weeks of separation for evaluation of the reproducibility of the measurements.

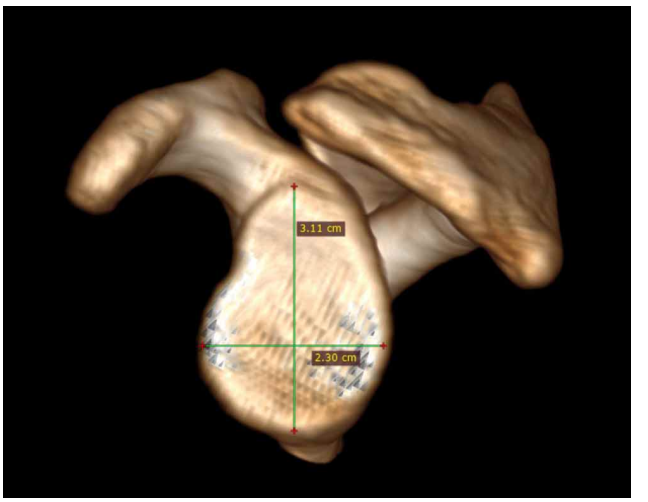

Fig. 1. Morphometric measurements. Two morphometric measurements were obtained: height and width. Glenoid height was measured as the maximum length from the upper pole of the glenoid (12 o'clock position) to the lower pole (6 o'clock position) and glenoid fossa width was measured as the maximum diameter in an orthogonal orientation to the previously measured height.

Statistical analysis. Data are presented as mean ± SD, and the coefficient of variation (CV) was calculated. The Kolmogorov-Smirnov test and Shapiro-Wilk were used to evaluate the normal distribution. A linear regression model was estimated considering the glenoid fossa width as the quantitative dependent variable and the glenoid height as the quantitative independent variable adjusted for age (quantitative) and sex (qualitative, binary). The adjusted R2 and the statistical significance of the regression coefficients were calculated with Student's t-test using Stata BE 17® software. A p-value of 0.05 was considered significant. In addition, the assumption of normal distribution of errors (Kolmogorov-Smirnov test), independence of errors (Durbin Watson test), and homoscedasticity were evaluated for model validation. The intraobserver and interobserver correlation were evaluated with the intraclass correlation coefficient (ICC). The study was reviewed and approved by the ethical committee at our institution.

RESULTS

The glenoid fossa width was 25.53 ± 2.41, and the glenoid height was 35.17 ± 3.25 in this sample (Table I). Analysis of the measured height and width values demonstrated a strong correlation of 0.8124 for the full cohort.

Table I. Variable values.

Variable	Obs.	Mean	Std. Dev.	VC	Min	Max
Height	101	35.17129	3.248456	9,24	27.8	42.6
Width	101	25.52772	2.41239	9,45	20.1	32
Age	101	51.9604	19.16138	37,75	15	88

Obs = Observations; Std. Dev. = Standard deviation; VC = Variability Coefficient; Min = Minimum; Max = Maximum.

A linear regression model was estimated (Fig. 2) resulting in the formula "Width = 10.97+ 0.02* Age + 0.41 * Height - 1.95 * Sex (1 = Female, 0 = Male)" (Fig. 3). This model presented all coefficients with p <0.05 and an adjusted R2 of 0.73. Furthermore, it fulfilled the assumption of linearity (Fig. 4), normal distribution of errors [Kolmogorov-Smirnov p > 0.05] (Fig. 5), independence of errors [Durbin-Watson d-statistic = 1.84] (Fig. 6), and homoscedasticity (Fig. 7). Regarding the predicted glenoid fossa widths, the regression formula from this CT data set produced a root mean squared error across all shoulders of 1.25 mm. The absolute error margin was 1.01 ± 0.71 mm (range: 0.038 to 3.608 mm) for the final formula.

Regarding the intraobserver correlation, ICC was 0.76 for height and 0.91 for width; the interobserver ICC was 0.93 for height and 0.86 for width.

Source	SS	df	MS		
Model	429.337718	3	143.112573	Prob > F	0.0000
Residual	152.624689	97	1.5734504	R-squared	0.7377
				Adj R-squared	0.7296
Total	581.962407	100	5.81962407	Root MSE	1.2544

Number of obs = 101
F(3, 97) = 90.95

Width	Coef.	Std. Err.	t	P>|t|	[95% Conf.	Interval]
Height	.4130915	.0533574	7.74	0.000	.3071918	.5189911
Age	.0201914	.0071426	2.83	0.006	.0060153	.0343675
Sex	-1.946338	.3675477	-5.30	0.000	-2.675819	-1.216857
_cons	10.97096	1.970683	5.57	0.000	7.059696	14.88222

Fig. 2. Linear regression model. SS = Sum of squares; df = Degrees of freedom; MS = Mean squared; obs = observations; F = F statistic; Prob > F = p-value for F statistic; Adj = Adjusted; MSE = Mean Squared Error; _cons = Intercept; Coef. = b coefficient; Std. Err. = Standard Error; t = t-student statistic; P>|t|= p-value for t statistic; Conf. Interval = Confidence interval; _cons = constant.

Glenoid width (mm) = 11 + 0,02 x Age (years) + 0,41 x Glenoid Height (mm) - 1,95 x sex (1 = Female, 0 = Male)

Fig. 3. Adjusted formula. Formula to calculate glenoid fossa width in relation to glenoid height, age, and sex.

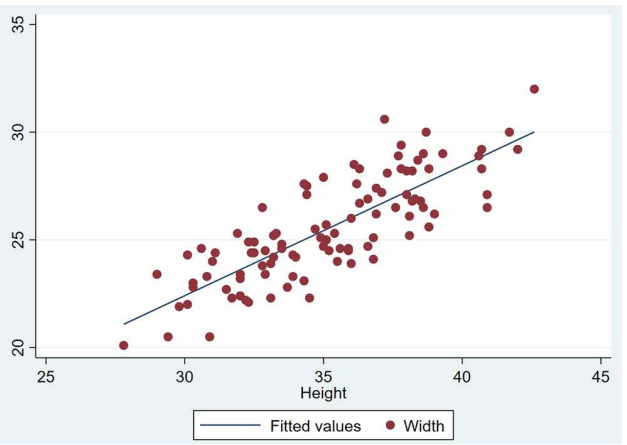

Fig. 4. Linearity assumption. The relationship between glenoid height and width is linear.

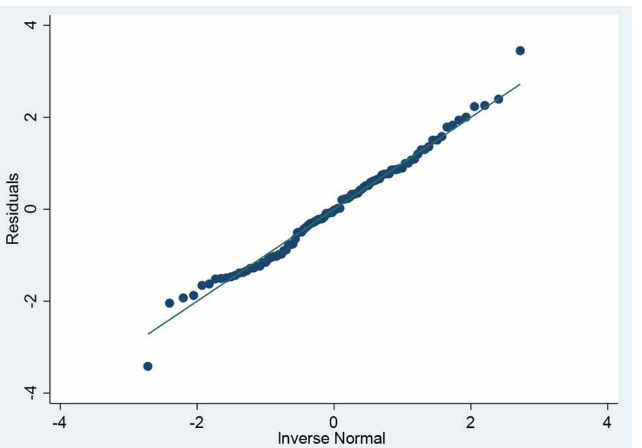

Fig. 5. Normality of errors assumption. The residuals normally distributed in this model. Kolmogorov-Smirnov's test was p > 0,05.

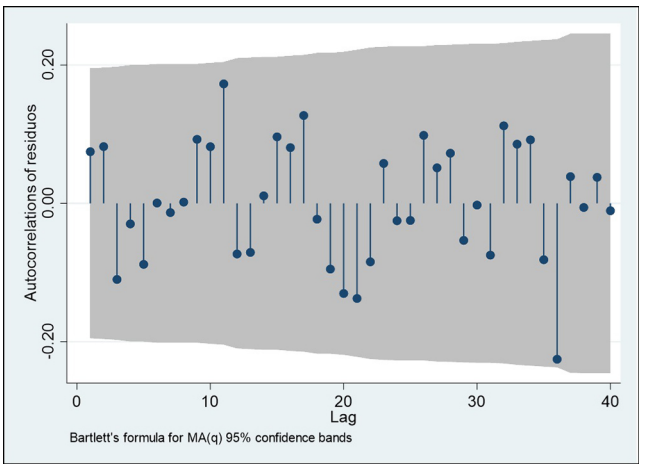

Fig. 6. Independence of errors assumption. The qualitative assessment (graph) rules out correlation between the residuals. The quantitative evaluation with Durbin-Watson d-statistic (1.839626) confirms the independence of errors by discarding the correlation of the residuals by presenting a value close to 2.

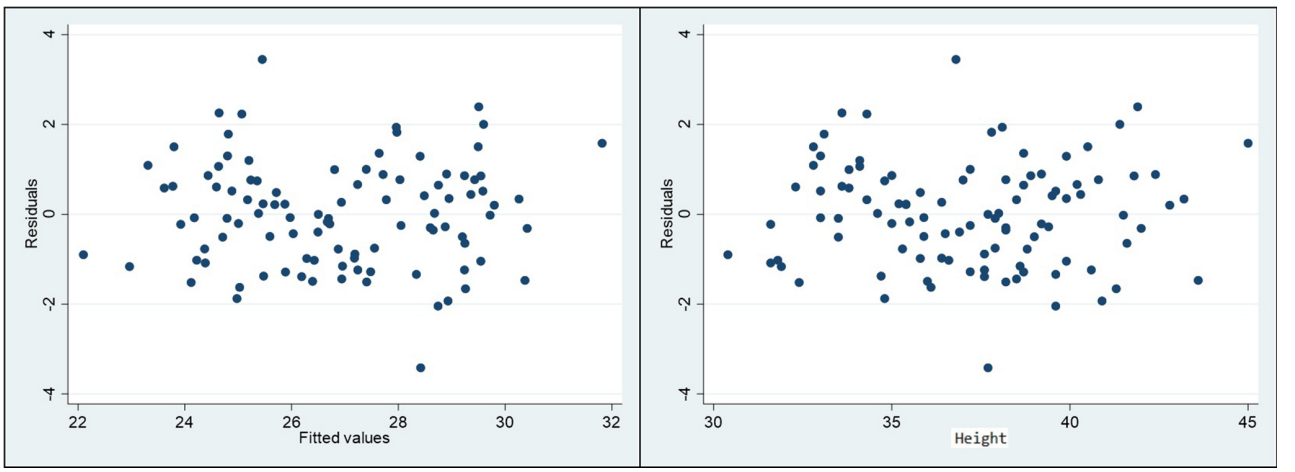

Fig. 7. Equal variances assumption (Homoscedasticity). The variance of the residuals is the same for all values of *x*.

DISCUSSION

The main finding of our study was a linear regression model that allows one to calculate the glenoid fossa width using the glenoid height adjusted for age and sex. The model is statistically significant, and it explains over 73 % of the correlation with the variables included and is based on reproducible and reliable measurements.

In 2015, Giles *et al*. declared that "…an inherent problem with the measurement of bone loss is that no true gold standard exists for comparison, as we are estimating the dimensions of a structure that is no longer present…". Even the use of the contralateral morphology does not allow one to establish a standard method of measurement. Several measurement methods are currently in use but there is no agreement on the ideal technique (Sugaya, 2014).

The data from our study confirmed the results of Giles and Owens whereby glenoid height and width are strongly correlated. In addition, we adjusted for age and sex to eliminate bias. Glenoid height is simply and reproducibly measured and is not compromised by glenohumeral instability (bone loss) allowing its use to estimate glenoid fossa width.

Regarding the study modality, the use of 2D images and the use of 3D reconstructions can affect the anatomical measurements at the glenoid level. In our anatomical review of the glenoid morphology in a CT scan (Contreras *et al*., 2020) using 2D images, we found that the glenoid size showed an average width of 26 ± 2.7 mm, a height of 40.3 ± 3.5 mm, and a vault depth of 26.5 ± 3.7 mm. Regarding the glenoid fossa width, the 2D measurement (26 ± 2.7 mm) and the 3D

measurement (25.53 ± 2.41) are similar, but the 2D (40.3 ± 3.5 mm) and 3D (35.17 ± 3.25) glenoid height measurement are different. This is probably associated with the measurement method because, according to Owens *et al*., the glenoid height is the maximum length from the upper pole of the glenoid (12 o'clock position) to the lower pole (6 o'clock position). In the 2D modality, the measurement is closer to the superior cortex of the supraglenoid tubercle, and thus it may be larger. This model must be used in 3D reconstructions because the use of another modality could lead to overestimations of the glenoid fossa width and therefore an overestimation of the glenoid deficit. This could affect the surgical decision. Giles *et al*. found similar results for glenoid height and width on CT (33.3 ± 2.9 mm and 26.2 ± 2.5 mm, respectively). Kubicka *et al*. (2016) compared 2D and 3D-CT in the assessment of glenoid bone loss and showed that 3D-CT reliability was nearly perfect in all measurements even if performed by an inexperienced observer.

In relation to the use of 3D reconstructions, it is important to consider that the true "en face" view is defined when the image displays the glenoid articular surface with its largest surface extension in the horizontal and vertical planes (Zhang *et al*.). Nevertheless, this definition is arbitrary and can lead to variability. Here, each evaluator subtracted the humeral head and the three-dimensional positioning of the glenoid in both measurements to obtain excellent intra and interobserver correlation; thus, the effect is probably minimal. Zhang *et al*. performed a quantitative description of a true "en face" view using the best-sphere fit method. However, we believe that this may complicate estimating the glenoid fossa width. Giles *et al*. found that intra-observer reliability was good to excellent with an ICC of 0.765 for glenoid fossa width and 0.992 for height (0.76 for height and 0.91 for width in our sample). Interobserver reliability also showed high levels of correlation with an ICC of 0.895 and 0.969 for width and height, respectively (0.93 for height and 0.86 for width in our sample).

Giles *et al*. found variations in glenoid size based on sex. Sex-specific regression analyses established that male and female formulas differ from the overall formula above but exhibit only an offset relative to each other similar to our sample with men presenting a 1.95 mm greater offset.

In relation to precision, we compared the prediction of the formula to the true glenoid fossa width values: a root mean squared error across all shoulders of 1.25 mm was calculated similar to the 1.2 mm obtained by Giles *et al*. The absolute error margin was 1.01. This low level of error indicates that the formulas used for the glenoid height predicted the glenoid fossa width exactly. This allows one to make decisions on the type of treatment with the greatest reproducibility.

In relation to other methods for estimation of glenoid fossa width, the reliability of the bare spot as a central reference point of the glenoid has been questioned. Saintmard *et al*. (2009) identified the bare spot in less than 48 % of cases during arthroscopy and in only 26 % with CT arthrography. Two cadaveric studies assessed bare spot measurements and showed that this is an unreliable landmark in glenoid measurements (Aigner *et al*., 2004; Huysmans *et al*., 2006). Surface measurement of the glenoid is probably the most popular method in clinical use and planning (Stefaniak *et al*.). The idea of a best-fit circle was developed by Sugaya *et al*. (2005) on 3D-CT. Baudi *et al*. (2005) developed the Pico method, which is based on calculating the size of the defect in the affected shoulder as a percentage of the best-fit circle area of the contralateral glenoid. However, the problem with all of these measurements is the lack of a gold standard for comparison.

Limitations of this study include that our sample had patients with a wide age range (15 to 88 years) including some that are beyond the average age group that presents anterior shoulder instability. However, all CT scans were analyzed for signs of degenerative changes (52.8 % of studies excluded); thus, the evaluated glenoid measurements should represent the normal anatomy. The formula was also adjusted for age.

CT ensures high resolution and is a gold standard in the assessment of chronic anterior shoulder instability allowing detection and quantification of the lesions (Lansdown *et al*., 2019), but one major disadvantage of a CT scan is the radiation dose. MRI is one solution: It has no ionizing radiation and is the most useful modality for soft tissue evaluation. However, it is much more expensive, less available, has longer scan times, and depends on technical quality.

The advantages of this study are the inclusion of a sample with many healthy subjects; the use of the gold standard imaging approach (3D-CT); measurement by expert and trained professionals; simple and reproducible measurements; robust statistical evaluation; and an easy-to-use formula applicable to clinical practice.

CONCLUSION

In conclusion, we found that glenoid height and width are strongly correlated. A 3D-CT specific formula was developed to predict glenoid fossa width based on height with sufficient accuracy to be clinically valuable. As such, the adjusted formula for 3D-CT in a Chilean sample is now described to assist surgeons in quantifying glenoid bone loss.

CONTRERAS, J.; OGRODNIK, C. & KHEK, P. Estimación del ancho de la fosa glenoidea para la pérdida ósea relacionada con inestabilidad con tomografía computarizada en una muestra chilena. *Int. J. Morphol., 39(5)*:1487-1492, 2021.

RESUMEN: La pérdida de hueso de la fosa glenoidea se ha asociado con recurrencia y falla después de la reparación del labrum glenoideo por inestabilidad del hombro. La cuantificación de la pérdida ósea glenoidea es fundamental para el tratamiento exitoso de la inestabilidad glenohumeral. El objetivo de este trabajo fue estimar un modelo de regresión lineal basado en la altura glenoidea en una tomografía computarizada ajustada por edad y sexo para calcular el ancho de la fosa glenoidea en una muestra chilena sana. Se revisaron las tomografías computarizadas de 101 hombros. La edad media fue de 51,96 años (DE 19,16; rango, 15-88 años) con 53 mujeres y 48 hombres. Se excluyeron los estudios con signos de pérdida ósea, inestabilidad, fractura o artritis. Después de la reconstrucción 3D-CT, se midió la altura y el ancho de cada fosa glenoidea utilizando la metodología de Owens. Todos los puntos de referencia para las 2 mediciones se colocaron en la superficie más lateral del margen glenoideo. Las mediciones de todos los hombros fueron registradas por 3 observadores y repetidas en un subconjunto (n = 20) de hombros, en condiciones ciegas, por el mismo observador, al menos 2 semanas después de las mediciones iniciales. La estadística descriptiva, la correlación intraclase y los coeficientes de regresión se calcularon con el software Stata BE 17®. Se consideró significativo un valor de p de 0,05. Se estimó un modelo de regresión lineal que resultó en la fórmula "Ancho = 10,97 + 0,02 * Edad + 0,41 * Altura - 1,95 * Sexo (1 = Mujer, 0 = Hombre)". Este modelo presentó todos los coeficientes con p <0.05 y un R2 ajustado de 0.73. Además, cumplió con los supuestos de linealidad, distribución normal de errores, independencia de errores y homocedasticidad. En cuanto a la correlación intraobservador, el CCI fue de 0,76 para la altura y 0,91 para la anchura; el ICC interobservador fue de 0,93 para la altura y 0,86 para la anchura. Se desarrolló una fórmula específica de 3D-CT para predecir el ancho glenoideo en función de la altura con suficiente precisión para ser clínicamente valiosa.

PALABRAS CLAVE: Articulación del glenohumeral; Fosa glenoidea; Anatomía; Luxación de hombro.

REFERENCES

Aigner, F.; Longato, S.; Fritsch, H. & Kralinger, F. Anatomical considerations regarding the "bare spot" of the glenoid cavity. Su*rg. Radiol. Anat., 26(4)*:308-11, 2004.

Apostolakos, J. M.; Wright-Chisem, J.; Gulotta, L. V.; Taylor, S. A. & Dines, J. S. Anterior glenohumeral instability: Current review with technical pearls and pitfalls of arthroscopic soft-tissue stabilization. *World J. Orthop., 12(1)*:1-13, 2021.

Baudi, P.; Righi, P.; Bolognesi, D.; Rivetta, S.; Rossi Urtoler, E.; Guicciardi, N. & Carrara, M. How to identify and calculate glenoid bone deficit. *Chir. Organi Mov., 90(2)*:145-52, 2005.

Burkhart, S. S. & De Beer, J. F. Traumatic glenohumeral bone defects and their relationship to failure of arthroscopic Bankart repairs: significance of the inverted-pear glenoid and the humeral engaging Hill-Sachs lesion. *Arthroscopy, 16(7)*:677-94, 2000.

Burkhart, S. S.; De Beer, J. F.; Tehrany, A. M. & Parten, P. M. Quantifying glenoid bone loss arthroscopically in shoulder instability. *Arthroscopy, 18(5)*:488-91, 2002.

De Filippo, M.; Schirò, S.; Sarohia, D.; Barile, A.; Saba, L.; Cella, S. & Castagna, A. Imaging of shoulder instability. *Skeletal Radiol., 49(10)*:1505-23, 2020.

Giles, J. W.; Owens, B. D. & Athwal, G. S. Estimating glenoid width for instability-related bone loss: A CT evaluation of an MRI formula. *Am. J. Sports Med., 43(7)*:1726-30, 2015.

Huysmans, P. E.; Haen, P.S.; Kidd, M.; Dhert, W. J. & Willems, J. W. The shape of the inferior part of the glenoid: a cadaveric study. *J. Shoulder Elbow Surg., 15(6)*:759-63, 2006.

Kubicka, A. M.; Stefaniak, J.; Lubiatowski, P.; D?ugosz, J.; Dzianach, M.; Redman, M.; Piontek, J. & Romanowski, L. Reliability of measurements performed on two dimensional and three dimensional computed tomography in glenoid assessment for instability. *Int. Orthop., 40(12)*:2581-8, 2016.

Lansdown, D. A.; Cvetanovich, G. L.; Verma, N. N.; Cole, B. J.; Bach, B. R.; Nicholson, G.; Romeo, A.; Dawe, R. & Yanke, A. B. Automated 3-dimensional magnetic resonance imaging allows for accurate evaluation of glenoid bone loss compared with 3-dimensional computed tomography. *Arthroscopy, 35(3)*:734-40, 2019.

Owens, B. D.; Burns, T. C.; Campbell, S. E.; Svoboda, S. J. & Cameron, K. L. Simple method of glenoid bone loss calculation using ipsilateral magnetic resonance imaging. *Am. J. Sports Med., 41(3)*:622-4, 2013.

Park, I.; Oh, M. J. & Shin, S. J. Effects of glenoid and humeral bone defects on recurrent anterior instability of the shoulder. *Clin. Orthop. Surg., 12(2)*:145-50, 2020.

Provencher, M. T.; Bhatia, S.; Ghodadra, N. S.; Grumet, R. C.; Bach Jr., B. R.; Dewing, C. B.; LeClere, L. & Romeo, A. A. Recurrent shoulder instability: current concepts for evaluation and management of glenoid bone loss. *J. Bone Joint Surg. Am., 92 Suppl. 2*:133-51, 2010.

Saintmard, B.; Lecouvet, F.; Rubini, A. & Dubuc, J. E. Is the bare spot a valid landmark for glenoid evaluation in arthroscopic Bankart surgery? *Acta Orthop. Belg., 75(6)*:736-42, 2009.

Stefaniak, J.; Lubiatowski, P.; Kubicka, A. M.; Wawrzyniak, A.; Wa?ecka, J. & Romanowski, L. Clinical and radiological examination of bony-mediated shoulder instability. EFORT Open Rev., 5(11):815-27, 2020.

Sugaya, H. Techniques to evaluate glenoid bone loss. *Curr. Rev. Musculoskelet. Med., 7(1)*:1-5, 2014.

Sugaya, H.; Moriishi, J.; Kanisawa, I. & Tsuchiya, A. Arthroscopic osseous Bankart repair for chronic recurrent traumatic anterior glenohumeral instability. *J. Bone Joint Surg. Am., 87(8)*:1752-60, 2005.

Willemot, L. B.; Elhassan, B. T. & Verborgt, O. Bony reconstruction of the anterior glenoid rim. *J. Am. Acad. Orthop. Surg., 26(10)*:e207-e218, 2018.

Zhang, H.; Zhu, Y.; Lu, Y.; Li, F. & Jiang, C. Establishment of a true en face view in the evaluation of glenoid morphology for treatment of traumatic anterior shoulder instability. *Arthroscopy, 36(3)*:668-79, 2020.

Corresponding author:
Dr. Julio Contreras Fernández
Avda. Pocuro #2170
Providencia
Santiago
CHILE

E-mail: juliocontrerasmd@gmail.com

Recibido : 23-06-2021
Aceptado: 24-07-2021.